

## MIT Open Access Articles

*Photoexcitation of the triplet exciton  
in single wall carbon nanotubes*

The MIT Faculty has made this article openly available. **Please share** how this access benefits you. Your story matters.

**Citation:** Alphenaar, Bruce W. et al. "Photoexcitation of the triplet exciton in single wall carbon nanotubes." Physical Chemistry of Interfaces and Nanomaterials VIII. Ed. Oliver L. A. Monti & Oleg V. Prezhdo. San Diego, CA, USA: SPIE, 2009. 739607-9. © 2009 SPIE--The International Society for Optical Engineering

**As Published:** <http://dx.doi.org/10.1117/12.827254>

**Publisher:** The International Society for Optical Engineering

**Persistent URL:** <http://hdl.handle.net/1721.1/52720>

**Version:** Final published version: final published article, as it appeared in a journal, conference proceedings, or other formally published context

**Terms of Use:** Article is made available in accordance with the publisher's policy and may be subject to US copyright law. Please refer to the publisher's site for terms of use.



# Photoexcitation of the triplet exciton in single wall carbon nanotubes

Bruce W. Alphenaar and Aditya D. Mohite

Dept. of Elec. & Comp. Eng., University of Louisville, Louisville, KY, 40292

Jagadeesh S. Moodera and Tiffany S. Santos

Francis Bitter Magnet Laboratory, MIT, Cambridge, MA, 02139

## ABSTRACT

The carbon nanotube photoexcitation spectrum is dominated by excitonic transitions, rather than interband transitions between continuum states. There are eight distinct excitonic transitions (four singlet and four triplet), each with two-fold degeneracy. Because the triplet excitons are spin polarized with electron and hole spins both pointing in the same direction, they are optically inactive, and optical spectroscopy has revealed no evidence for their existence. Here, we show that by the interaction with a spin filter ferromagnetic semiconductor, photoexcitation of the carbon nanotube triplet exciton is possible, and its contribution to the photocurrent can be detected. The perturbation provided by the spin filter allows for inter-system mixing between the singlet and triplet excitonic states, and relaxes the spin selection rules. This supplies the first evidence for the existence of the triplet exciton, and provides an avenue for the optical excitation of spin polarized carriers in carbon nanotubes.

## INTRODUCTION

Single wall carbon nanotubes are an ideal platform for probing one-dimensional spin transport. They provide a gateable, nanoscale channel for the transport and manipulation of electron spin over relatively large distances. A major challenge, however, remains the reliable injection of spin polarized carriers into carbon nanotubes. Ferromagnetic contacting schemes have been somewhat successful for this purpose<sup>1</sup>, but the yield for working spin injecting contacts is very low. As a result, the existing evidence for electrical spin injection in carbon nanotubes remains sparse and controversial. A method to optically inject electron spin in carbon nanotubes would solve many of the problems associated with electrical spin injection. In GaAs and other III/V materials, spin polarized carriers can be efficiently generated by photoexcitation with circularly polarized light<sup>2</sup>. Optically excited spin transitions are possible in III/V materials because spin-orbit coupling mixes the spin with the electron orbital motion. In carbon nanotubes, however, spin orbit coupling is very weak (as it is in most organic materials). Spin-orbit mixing in carbon nanotubes can only be observed at milli-Kelvin temperatures and in pristine samples<sup>3</sup>. Consequently, photoexcitation is not expected to be an efficient means of producing spin polarized carriers.

Nanotubes also differ from III/V materials in that the photoexcitation spectrum is dominated by excitonic transitions, rather than by interband transitions between continuum states<sup>4,11</sup>. Single wall nanotubes have two k-space valleys, known as the K and K' points. Together with the electron spin, this produces eight distinct excitonic transitions (four singlet and four triplet), each with two-fold degeneracy. Figure 1(a) shows the three lowest lying carbon nanotube excitonic transitions (<sup>1</sup>E<sub>11</sub>, <sup>1</sup>D<sub>11</sub>, and <sup>3</sup>E<sub>11</sub>) along with the ground interband transition (S<sub>11</sub>). The <sup>1</sup>E<sub>11</sub> transition is the only optically active exciton<sup>10</sup>. It is a singlet exciton derived from a bonding-like combination of the K-point and K'-point states, and forms the dominant optical transition observed in nanotubes under normal experimental conditions. The <sup>1</sup>D<sub>11</sub> transition (the so-called dark exciton) is the singlet exciton derived from the anti-bonding like combination of the K-point and K'-point states. It has even parity, so it is dipole forbidden, but can become optically active under the application of high magnetic fields<sup>8,12</sup>. In addition to the singlet excitons, there exists a complimentary set of triplet excitons<sup>13</sup>. Figure 1(a)

shows the  $^3E_{11}$  triplet exciton, which (like the  $^1E_{11}$  singlet exciton) is derived from the bonding-like combination of the K-point and K'-point states. In contrast with the singlet excitons, which have zero-net spin, the triplet excitons are spin polarized with electron and hole spins both pointing in the same direction. Having finite spin, they should be optically inactive, and optical spectroscopy has revealed no evidence for their existence.

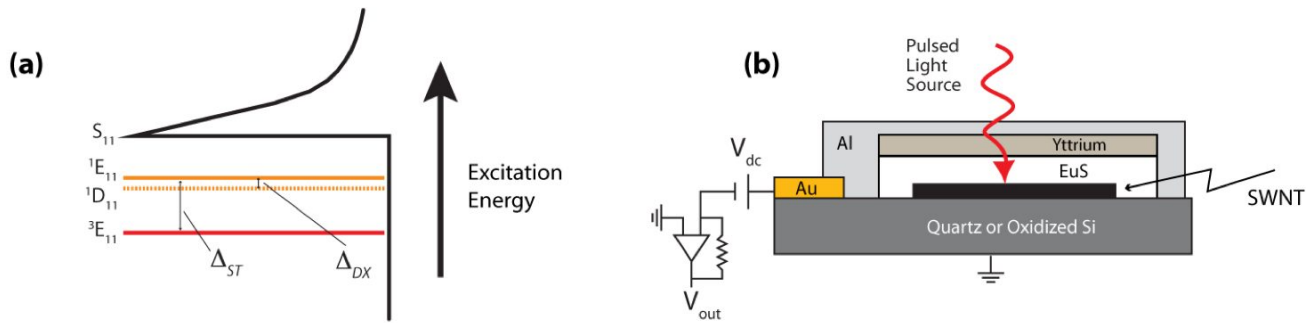


**Figure 1 a.** Excitation energy diagram showing the three lowest energy excitonic transitions ( $^1E_{11}$ ,  $^1D_{11}$ ,  $^3E_{11}$ ), along with the lowest lying band-to-band transition ( $S_{11}$ ).  $^1E_{11}$  and  $^3E_{11}$  are singlet and triplet excitons, respectively, corresponding to the bonding like combination of the K-point and K'-point states.  $^1D_{11}$  is the so-called dark exciton, corresponding to the anti-bonding like combination of the K-point and K'-point states. Also shown are the light-dark ( $\Delta_{DX}$ ) and singlet-triplet ( $\Delta_{ST}$ ) zero-field energy splitting. **b.** Schematic diagram of the device configuration used in the capacitive photocurrent measurements. The single wall nanotube (SWNT) is grown on an oxidized silicon or quartz substrate and coated with a EuS / yttrium tunnel barrier, followed by an aluminum contact. Pulsed laser light is directed at the nanotube, and the resulting ac signal  $V_{out}$  is amplified and measured. A dc bias  $V_{dc}$  is applied to encourage exciton dissociation.

In this paper, we show that under paramagnetic perturbation, photoexcitation of the carbon nanotube triplet exciton is possible, and its contribution to the photocurrent can be detected. Carbon nanotubes are coated with EuS, a spin filtering material that couples with the nanotube excitonic states. The perturbation provided by the EuS allows for inter-system mixing between the singlet and triplet excitonic states, and relaxes the spin selection rules for optical absorption into the triplet exciton. Alignment of the spin states in the EuS results in the appearance of an additional peak in the nanotube photocurrent spectrum, associated with the lowest energy triplet excitation. The peak lies well below the singlet peak in energy, at a much larger energy separation than what has been observed for the singlet dark exciton state. The triplet peak height increases in magnitude as the spin alignment is rotated with respect to the nanotube axis, while the singlet peak remains unchanged. This supplies the first evidence for the existence of the triplet exciton in individual single wall nanotubes, and provides an avenue for the optical excitation of spin polarized carriers in carbon nanotubes.

## EXPERIMENT

The device structure used in our experiments is shown in Figure 1(b). CVD grown carbon nanotubes (1.3 nm to 2.1 nm in diameter) are randomly distributed on an oxidized silicon substrate, with a coverage of approximately 1 nanotube / 100  $\mu\text{m}^2$ . Nanotubes are grown on either quartz or oxidized silicon substrates using the chemical vapor deposition method. A solution of iron (III) nitrate in isopropyl alcohol is dispersed on the substrate by dipping the sample in the catalyst solution followed by a hexane rinse. The samples are then heated in a tube furnace to 890°C. Reduction of the catalyst particles is done by flowing hydrogen argon gas at 100 sccm, after which the nanotubes are grown using methane gas at 100 sccm for 5-7 minutes. Nanotube distribution and diameter is determined using a combination of atomic force microscopy and Raman spectroscopy. In analyzing the Raman spectra, the relation  $\omega_{RBM} = A/d + B$ , is used, where  $A = 234 \text{ cm}^{-1}$ ,  $B = 10 \text{ cm}^{-1}$ ,  $\omega_{RBM}$  is the radial breathing mode, and  $d$  is the nanotube diameter.

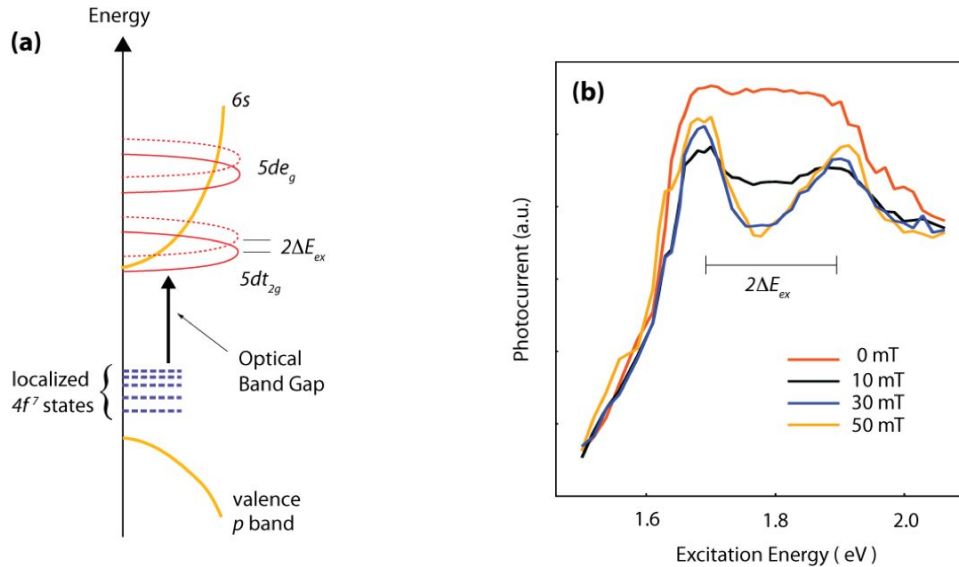


**Figure 2 a.** Energy diagram of europium sulfide (EuS). Spin polarization of the localized  $4f^7$  states results in an exchange splitting  $2\Delta E_{ex}$  of the  $5dt_{2g}$  states forming the conduction band. The optical band gap is determined by the energy separation between the  $4f^7$  states and the  $5dt_{2g}$  states. **b.** Capacitive photocurrent spectrum of the EuS film for four different applied fields. Field is applied parallel to the EuS film. The exchange splitting  $2\Delta E_{ex}$  becomes visible as the magnetic field increases to 10 mT. Above 30 mT, the EuS magnetization is complete, and the spectrum no longer changes with increasing magnetic field.

The nanotubes are then coated with a 3 nm thick layer of EuS, followed by a 3 nm thick yttrium protective layer, and a 6 nm thick aluminum contact. EuS films are prepared in a high vacuum deposition chamber with a base pressure of  $6 \times 10^{-8}$  torr. The EuS layer is deposited at room temperature by e-beam evaporation from a EuS pellet. The over layers of Y, Al, and Au are subsequently deposited. Appropriate shadow metal masks are utilized to create EuS film and the Au electrodes away from the quartz/oxidized silicon substrate edges, with the partial overlap of the Au with Al/Y/EuS as shown in Fig. 1(b). A thin layer of  $Al_2O_3$  deposited over the whole area protects the structure. The entire sample is prepared in situ.

Optical characterization is performed using a recently developed capacitive photocurrent technique<sup>14-18</sup>. The sample is fixed to a copper block within an optical flow cryostat which is placed between the poles of an electromagnet. Tunable pulsed laser light is directed through the thin Al/Yt/EuS contact layer and onto the carbon nanotubes. The light source is a Spectra-Physics optical parametric amplifier (OPA) pumped by a 130 fs pulsed Ti: Sapphire laser with a repetition rate of 1 kHz. If electron-hole pairs are generated in the carbon nanotube (or in the EuS), and dissociate into the Al contact, an additional potential is measured at the Al contact. The signal strength is proportional to the excited charge density multiplied by the charge separation distance. By keeping the laser spot size smaller than the nanotube separation distance, individual nanostructures can be probed. The wavelength resolution and sensitivity obtained is similar to a standard photo-absorption measurement.

Capacitive photocurrent measurements were first made on an EuS film with no carbon nanotube present. EuS is one of the europium chalcogenides, a wide-band gap semiconductor that undergoes a ferromagnetic transition at cryogenic temperatures.<sup>19-20</sup> Europium chalcogenides were studied extensively during the 1960s and 1970s, and have recently found application as spin filtering materials. The energy diagram for EuS is shown in Fig. 2(a). The gap between the  $4f^7$  states and the  $5dt_{2g}$  states define the optical band gap. Below a temperature of 16.6 K, the half-filled  $4f^7$  states become ferromagnetically ordered. Exchange interaction in turn causes the conduction band to split into two energy levels, separated by the exchange energy  $2\Delta E_{ex}$ . Figure 2(b) shows the capacitive photocurrent spectrum of an EuS film on an oxidized silicon substrate, cooled in zero magnetic field to a temperature of 8°K. The photocurrent increases sharply at an excitation energy of about 1.5 eV, which marks the optical band gap.<sup>21</sup> When the magnetic field is increased to 30 mT, a dip appears in the photocurrent trace, forming two peaks which correspond to the up and down spin levels of the  $5dt_{2g}$  states.

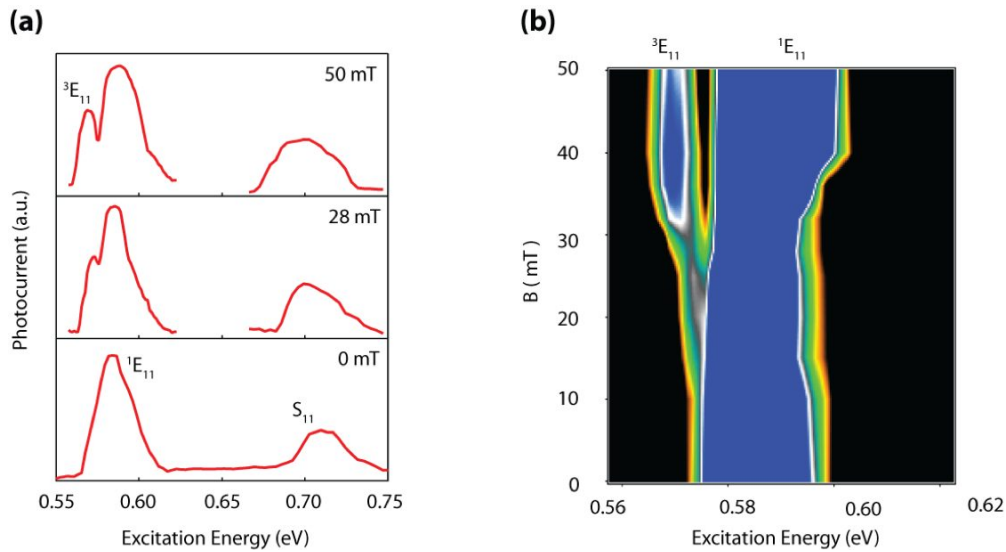


**Figure 3 a.** Capacitive photocurrent spectra of a EuS coated single wall nanotube for three different applied magnetic fields. Field is applied parallel to the EuS film, and no effort was made to align the field direction with the nanotube axis. At zero field, peaks are observed corresponding to the light singlet ( $^1E_{11}$ ) and interband ( $S_{11}$ ) transitions. As the field increases, the EuS is magnetized, causing a new peak to appear, corresponding to the  $^3E_{11}$  triplet transition. The field also causes the  $S_{11}$  transition to shift, presumably due to the Aharonov Bohm flux through the tube. **b.** Image plot showing the emergence of the triplet exciton peak with increasing magnetic field. The plot was formed from a series of photocurrent spectra obtained at different magnetic fields.

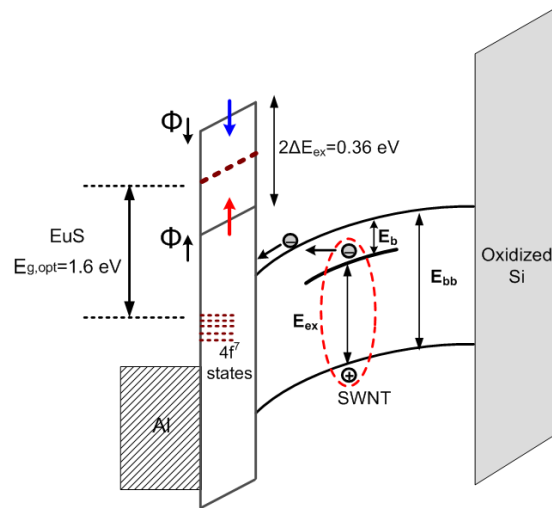


**Figure 4** The interband ( $E_{bb}$ ) and bound exciton ( $E_{ex}$ ) transition energies are indicated for an individual nanotube within the Al / EuS / SWNT / dielectric capacitor. A built-in potential exists at the EuS / SWNT interface due to the difference in work functions between the SWNT and EuS, and to the particular distribution of trapped charge existing at the interface. A bias  $V_{dc}$  applied across the capacitor can be used to vary the magnitude of the electric field, and hence the band bending at the EuS/SWNT interface. Under illumination, photon absorption results in the excitation of an electron from the ground state to form an electron-hole pair in the nanotube. If the excited charge carriers are free to move, the band bending at the EuS / SWNT interface will result in separation of the positive and negative charge, and a measurable displacement current across the capacitor. If, however, the photo-excited carriers form an exciton state, no displacement current will be measured unless the exciton first dissociates into available free carrier states.

Next, we consider the capacitive photocurrent spectrum of individual carbon nanotubes coated with the EuS film (Fig. 3). Because the excitation energy is tunable from 0.4-4 eV, it is possible to observe both the EuS and nanotube spectra at a single laser position. The nanotubes are located by first setting the excitation energy to the  $^1E_{11}$  transition energy, (approximately 0.6 eV for a 1.6 nm diameter nanotube), and then searching for a response in the capacitive photocurrent while scanning the laser spot over the sample surface. During the measurement, a bias of 10 V is applied between the contact and substrate ground to encourage exciton dissociation. Once a signal is detected, the laser polarization is rotated to maximize the signal, and to ensure that only a single nanotube is being measured (see Ref. 14). If more than one nanotube is present, additional photocurrent peaks will appear as the polarization aligns with the various nanotube axes.

Diameter (nm)	$^1E_{11}$ (meV)	$^3E_{11}$ (meV)	$S_{11}$ (meV)	$\Delta_{ST}$ (meV)	$S_{11} - ^1E_{11}$ (meV)
1.44	611	588	866	23	255
1.5	573	553	680	20	107
1.63	586	569	710	17	124
1.82	729	715	-----	14	-----

**Table 1** The singlet ( $^1E_{11}$ ), triplet ( $^3E_{11}$ ), interband ( $S_{11}$ ), singlet-triplet splitting ( $\Delta_{ST}$ ) and singlet exciton binding energy ( $S_{11} - ^1E_{11}$ ) for four different diameter EuS coated single wall nanotubes. The diameter is estimated from the average diameter of 15 nanotubes whose Raman spectra is taken for each sample.

The sample is first cooled to 8°K at zero magnetic field to randomly orient the spins of the EuS. In this configuration, the nanotube photocurrent spectrum is indistinguishable from that measured without the EuS being present.<sup>14</sup> As shown in the bottom panel of Fig. 3(a), two photocurrent peaks are observed, corresponding to the  $^1E_{11}$  exciton transition, and the interband  $S_{11}$  transition, respectively. The peak assignment is made by comparing the bias dependence of the two peaks. The excitonic peak height ( $^1E_{11}$ ) increases sharply with increasing bias, while the interband transition ( $S_{11}$ ) shows no bias dependence. Note that the  $S_{11}$  and  $^1E_{11}$  peak heights are comparable in magnitude. This is in contrast to nanotube absorption or luminescence measurements where the excitonic transition is completely dominant over the interband transition. As shown in Fig. 4, the ease with which free carriers are collected by the contact compensates for the relatively low oscillator strength of the interband transition.

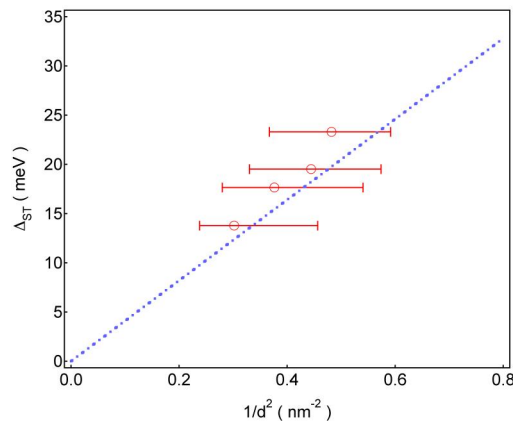


**Figure 5** The measured singlet triplet splitting ( $\Delta_{ST}$ ) for each of the four measured EuS coated single wall nanotubes versus  $1/d^2$ . The error bars show the range of diameters out of the 15 measured for each sample, while the points show the average diameter. The dashed line is the theoretical prediction for the singlet-triplet splitting taken from Ref. 27.

Next, a small magnetic field is applied to align the spins in the EuS film. This results in the appearance of a new, low energy peak. The new peak grows with increasing magnetic field, until spin alignment in the EuS is complete at 30 mT.

The field also causes the interband  $S_{11}$  peak to red shift by about 6 meV. This shift is most likely due to the magnetization of the EuS contact, which produces an Aharonov Bohm flux along the nanotube axis.<sup>22</sup> Assuming a standard value for the AB shift of 1 meV per telsa<sup>19</sup>, this implies that the EuS generates a field of approximately 6 T, and gives a relative permeability for EuS of around 200, in agreement with previously measured values.<sup>23</sup> Figure 3(b) is an image plot detailing the emergence of the new peak with increasing field. No obvious shift in the  ${}^1E_{11}$  peak position is observed, although some broadening does occur. Similar results were observed in measurements of four different nanotubes, taken from four different growth runs. The peak positions for each of the measured nanotubes are listed in Table 1.

## DISCUSSION

The emergence of the low energy peak indicates that the alignment of the spins in the EuS causes either the dark exciton  ${}^1D_{11}$  or the triplet exciton  ${}^3E_{11}$  lying below  ${}^1E_{11}$  to become optically active. It can be shown, however, that the dark exciton does not have the correct energy or magnetic field dependence to explain the new peak. Srivastava et al.<sup>12</sup> demonstrated that the dark-light energy splitting  $\Delta_{ld}$  is given by:

$$\Delta_{ld}^2 = \Delta_{DX}^2 + \left( \mu\pi d^2 B_{\parallel} / 4 \right)^2 \quad (1)$$

Here,  $\Delta_{DX}$  is the zero field splitting,  $\mu$  is a coupling constant (ranging from 0.4-1.0 meV / T-nm<sup>2</sup>)  $d$  is the nanotube diameter, and  $B_{\parallel}$  is the magnetic field pointing parallel to the nanotube axis. The zero field splitting  $\Delta_{DX}$  has a 1/d dependence, decreasing from 4 meV to 1 meV as the tube diameter increases from 1 nm to 1.3 nm. This suggests that in our larger diameter (1.3 nm to 2.1 nm) nanotubes  $\Delta_{DX}$  should be less than 1 meV. The measured energy splitting, however, is more than an order of magnitude larger than this, ranging from 14 meV to 23 meV (see Fig. 5). To achieve this would require a magnetic field of between 100 T and 300 T, much larger than the field produced by the EuS.<sup>24,25</sup> Some of this difference could be due to the dielectric medium in which the nanotube is located.<sup>26</sup> (Our samples are grown on oxidized silicon while those of Ref. 12 are micelle encapsulated tubes on quartz.) However, the  ${}^1E_{11}$  values we observe (0.73-0.57 eV for 1.3-2.1 nm diameter tubes) follow the same 1/d dependence as those observed in Ref. 12 (1.1-0.8 eV for 1.0-1.3 nm diameter nanotubes) suggesting that the dielectric constants are not substantially different between the two experiments. The observed order of magnitude increase in  $\Delta_{DX}$  is difficult to account for in this way, and can more easily be described by the predicted singlet-triplet energy spacing.<sup>27</sup>

In addition to the wrong energy spacing, the dark exciton also has the wrong magnetic field dependence to explain the new peak. As seen in Eq. 1, the light-dark splitting is strongly dependent on the orientation of the magnetic field with respect to the nanotube axis. To test for this effect in the EuS coated nanotubes, we employ the measurement set-up shown in Fig. 4(a). A permanent niodymium ring magnet is placed behind the sample. The magnetic orientation of the EuS contact can then be rotated with respect to the carbon nanotube axis by rotating the orientation of the fixed magnet. The results are shown in Fig. 4(b). The magnitude of the low energy peak increases by a factor of 3 as the magnetic field is rotated to lie parallel to the nanotube axis. The maximum peak height thus occurs as the EuS magnetization aligns with the natural spin orientation of the carbon nanotube. However, the splitting between the two peaks, as well as the magnitude of the  ${}^1E_{11}$  peak remain constant. This is not what would be expected for the magnetic field orientation dependence of the light-dark splitting (as observed in Ref. 12) We must therefore conclude that the new peak is instead due to the  ${}^3E_{11}$  triplet exciton.

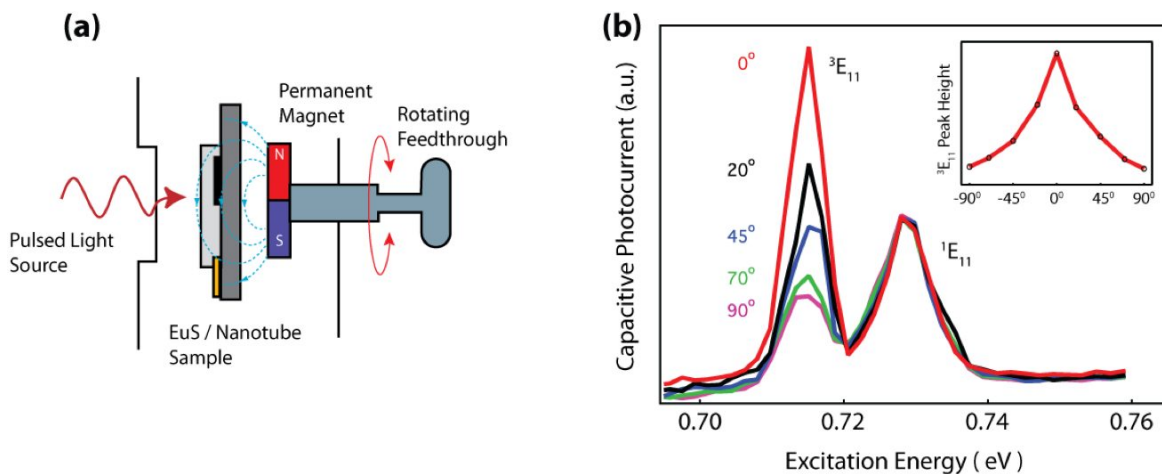


**Figure 6 a.** Measurement configuration used to rotate the polarization of the spin orientation in the EuS film. A permanent neodymium ring magnet is placed behind the sample, and rotated with respect to the nanotube axis. **b.** Capacitive photocurrent as a function of magnetic orientation. The  ${}^3E_{11}$  triplet peak grows as the field is oriented parallel to the nanotube axis. The  ${}^1E_{11}$  singlet peak, and the singlet-triplet energy spacing remain unchanged. Inset shows the  ${}^3E_{11}$  peak height as a function of magnetic field orientation.

## CONCLUSIONS

In a variety of systems, mixing between the singlet and triplet states has been induced by the large orbital angular momentum of a heavy metal compound.<sup>28-30</sup> For example, iridium compounds are used to induce singlet-triplet decay in conjugated polymers.<sup>31</sup> It is possible then that the close proximity of the heavy Eu atoms to the nanotube induces singlet-triplet mixing among the nanotube excitonic states. This hypothesis implies that the EuS is merely a source for spin orbit coupling, which could also be provided by any number of heavy metal compounds. In fact, heavy metals (i.e., Au, Ti, Pt, and Pd) are typically used to make contact to carbon nanotubes. Despite this, no previous evidence for the triplet peak has been observed<sup>32</sup>.

An alternative mechanism for triplet enhancement is exchange interaction between the nanotube and EuS states. This mechanism has been shown to apply for an aromatic molecule (M) in the presence of a paramagnetic molecule (such as O<sub>2</sub> or NO<sub>2</sub>)<sup>33-35</sup>. The ground state of O<sub>2</sub> is a triplet state, with two spin polarized electrons.<sup>36</sup> For small separations between M and O<sub>2</sub>, coupling occurs between the singlet and triplet excitations ( ${}^1M_{11}$  and  ${}^3M_{11}$ ), and the oxygen ground state. Exchange interactions induces strong mixing between the two coupled states. This allows the triplet state of the uncoupled molecule  ${}^3M_{11}$  to take on some of the singlet character of  ${}^1M_{11}$ . In our case, the nanotube singlet ( ${}^1E_{11}$ ) and triplet ( ${}^3E_{11}$ ) states can couple with the localized spin polarized ground state occupied by the 4f<sup>7</sup> electrons of the Eu<sup>2+</sup> magnetic ions in the EuS<sup>25</sup>. Once again, there will be strong exchange interactions mixing the coupled states, depending on the orientation of the electron spins in the EuS/nanotube complex. This coupling will allow the  ${}^3E_{11}$  state to take on some of the singlet character of the  ${}^1E_{11}$ , causing enhancement in the absorbance. Calculations are required to confirm the existence of this effect in the EuS coated nanotubes.

The method presented here can be applied to other excitonic systems which are limited by the ability to optically excite and detect the triplet exciton, such as organic photovoltaic materials. In this way, improvement of the photocurrent efficiency due to additional absorption into the triplet exciton could be achieved<sup>37</sup>. In addition, the method provides a mechanism for the optical injection of spin polarized electron hole pairs in carbon nanotubes and other nanoscale structures. Optical spin injection has been highly successful for III/V semiconductors<sup>2</sup>, but carbon nanotube spin electronics has been forced to rely on low yield ferromagnetic contacting schemes<sup>1</sup>. The EuS contact can also be used as a means to filter spin polarized electrons for spin injection and detection.



## ACKNOWLEDGEMENTS

The authors acknowledge Dr. Sergei Tretiak for theoretical guidance. Financial support is provided by the Office of Naval Research ONR N00014-06-1-0228 and ONR N00014-06-1-0235, the National Science Foundation NSF DMR 0504158 and the U.S. Department of Energy DE-FG02-07ER46375.

## REFERENCES

- [1] Tsukagoshi, K., Alphenaar, B.W. and Ago, H., "Coherent transport of electron spin in ferromagnetically contacted carbon nanotubes," *Nature* 401, 572-574 (1999).
- [2] Pierce, D.T. et al., "GaAs spin polarized electron source," *Rev. Sci. Instrum.* 51, 478-499 (1980).
- [3] Kuemmeth, F., Ilani, S., Ralph, D.C., and McEuen, P.L., "Coupling of spin and orbital motion of electrons in carbon nanotubes," *Nature* 452, 448-452 (2008).
- [4] Ando, T., "Excitons in carbon nanotubes," *J. Phys. Soc. Jpn.* 66, 1066-1073 (1997).
- [5] Wang, F., Dukovic, G., Brus, L.E. and Heinz, T.F., "Optical resonances in carbon nanotubes arise from excitons," *Science* 308, 838-841 (2005).
- [6] Maultzsch, J. et al., "Exciton binding energies in carbon nanotubes from two-photon photoluminescence," *Applied Physics Letters* 72, 241402 (2005).
- [7] Zhao, H. and Mazumdar, S., "Electron-electron interaction effects on the optical excitations of semiconducting single-walled carbon nanotubes," *Physical Review Letters* 93, 157402 (2004).
- [8] Ando, T., "Effects of valley mixing and exchange on excitons in carbon nanotubes with Aharonov-Bohm flux," *J. Phys. Soc. Jpn.* 75, 024707 (2006).
- [9] Spataru, C.D., Ismail-Beigi, S., Benedict, L.X. and Louie, S.G., "Excitonic effects and optical spectra of single-walled carbon nanotubes," *Physical Review Letters* 92, 077402 (2004).
- [10] Perebeinos, V., Tersoff, J. and Avouris, P., "Radiative lifetime of excitons in carbon nanotubes," *Nano Letters* 5, 2495-2499 (2005).
- [11] Barros, E.B. et al., "Selection rules for one- and two-photon absorption by excitons in carbon nanotubes," *Phys. Rev. B* 73, 241406(R) (2006).
- [12] Srivastava, A., Htoon, H., Klimov, V. I. and Kono, J., "Direct observation of dark excitons in individual carbon nanotubes: Inhomogeneity in the exchange splitting," *Phys. Rev. Lett.* 101, 087402 (2008).
- [13] Tretiak, S., "Triplet state absorption in carbon nanotubes: A TD-DFT study," *Nano Letters* 7, 2201-2206 (2007).
- [14] Mohite, A.D., Gopinath, P., Shah, H.M. and Alphenaar, B.W., "Exciton dissociation and Stark effect in the carbon nanotube photocurrent spectrum," *Nano Letters* 8, 142-146 (2008).
- [15] Mohite, A., Lin, J.-T., Sumanasekera, G. and Alphenaar, B. W., "Field enhanced photocurrent spectroscopy of excitonic states in single-wall carbon nanotubes," *Nano Letters* 6, 1369-1373 (2006).
- [16] Mohite, A. D. et al., "Photocurrent spectroscopy of double-wall carbon nanotubes," *Chem. Phys. Lett.* 412, 190 (2005).
- [17] Mohite, A., Gopinath, P., Chakraborty, S., and Alphenaar, B.W., "Displacement current detection of photoconduction in carbon nanotubes," *Appl. Phys. Lett.* 86, 061114 (2005).
- [18] Vaddiraju, S., et al., "Mechanism of 1D crystal growth in reactive vapor transport: indium nitride nanowires," *Nano Letters* 5, 1625 (2005).
- [19] Moodera, J.S., Santos, T.S., and Nagahama, T., "The phenomena of spin-filter tunneling," *J. Phys. Condens. Matter* 18, 1-24 (2006).

- [20] Mauger A. and Godart C., "The magnetic, optical, and transport properties of representatives of a class of magnetic semiconductors: the europium chalcogenides," *Phys. Rep.* 141, 51-176 (1986).
- [21] Dimmock, J.O., "Optical properties of the europium chalcogenides," *IBM J. Res. Develop.* 14, 301-308 (1970).
- [22] Ajiki, H. and Ando, T., "Electronic states of carbon nanotubes," *J. Phys. Soc. Jpn.* 62, 1255-1266 (1993).
- [23] Zaric S. et al., "Excitons in carbon nanotubes with broken time-reversal symmetry," *Phys. Rev. Lett.* 96, 016406 (2006).
- [24] McGuire, T.R., "Magnetic properties of some divalent europium compounds," *J. Appl. Phys.* 34, 1345-1346 (1963).
- [25] Hao, X., Moodera, J.S. and Meservey, R., "A thin film superconductor in an exchange field," *Phys. Rev. Lett.* 67, 1342-1345 (1991).
- [26] Ohno, Y. et al., "Excitonic transition energies in single walled carbon nanotubes: dependence on environmental dielectric constant," *Phys. Stat. Sol. B* 244, 4002-4005 (2007).
- [27] Capaz, R.B., Spataru, C.D., Ismail-Beigi, S. and Louie, S.G., "Excitons in carbon nanotubes: Diameter and chirality trends," *Phys. Stat. Sol. (b)* 244, 4016-4020 (2007).
- [28] Kavarnos, G., Cole, T., Scribe, P., Dalton, J. and Turro, N., "External heavy-atom induced spin-orbital coupling. Spectroscopic study of naphthonorbornanes," *JACS* 93, 1032-1034 (1971).
- [29] Romanova, Z., Deshayes, K. and Piotrowiak, P., "Remote intermolecular 'Heavy-Atom effect': spin-orbit coupling across the wall of a hemispherical," *J. Am. Chem. Soc.* 123, 2444-2445 (2001).
- [30] Hu, B., Wu, Y., Zhang, Z., Dai, S. and Shen, J., "Effects of ferromagnetic nanowires on singlet and triplet exciton fractions in fluorescent and phosphorescent organic semiconductors," *Appl. Phys. Lett.* 88, 022114 (2006).
- [31] Shao, Y. and Yang, Y., "Efficient organic heterojunction photovoltaic cells based on triplet materials," *Adv. Mater.* 17, 2841-2844 (2005).
- [32] Freitag, M., Martin, Y., Misewich, J.A., Martel, R. and Avouris, P.H., "Photoconductivity of single carbon nanotubes," *Nano Letters* 3, 1067-1071 (2003).
- [33] Hoijtink, G.J., "The influence of paramagnetic molecules on singlet-triplet transitions," *Mol. Phys.* 3, 67-70 (1960).
- [34] Murrell, J.N., "The effect of paramagnetic molecules on the intensity of spin-forbidden absorption bands of aromatic molecules," *Mol. Phys.* 3, 319-329 (1960).
- [35] Evans, D.F., "Magnetic perturbation of singlet-triplet transitions," *J. Chem. Soc.* 1, 3885-3888 (1957).
- [36] Kearns, D.R., "Physical and chemical properties of singlet molecular oxygen," *Chem. Rev.* 71, 395-427 (1971).
- [37] Hu, X. and Hu, B., "Photovoltaic processes of singlet and triplet excite states in organic solar cells," *Adv. Funct. Mater.* 18, 2611-2617 (2008).